NANO EXPRESS

High-Q Fano Resonance in Terahertz Frequency Based on an Asymmetric Metamaterial Resonator

Qin Xie[1], Guang-Xi Dong[1], Ben-Xin Wang[1*] and Wei-Qing Huang[2]

Abstract

We propose a planar metamaterial formed by four-strip metallic resonators, which can achieve high-Q Fano resonance in terahertz regime. This terahertz planar metamaterial supports a sharp Fano resonance at 0.81 THz with 25% transmission. The resonance bandwidth of the dip is 0.014 THz with the Q-factor of 58. The interference between the bright mode and dark mode leads to the Fano line shape. This sharp Fano profile is explained by the electromagnetic theory of Fano resonance. Moreover, multiple Fano resonances can be realized by adding more strips into the original structure. As an example, two Fano dips with Q-factors of 61 and 65 can be achieved via a five-strip structure.

Keywords: Metamaterial, Fano, Terahertz, Sensing

Background

Metamaterial is a kind of artificial material exhibiting exotic properties, such as negative refractive index [1] and ultra-high refractive index [2], which cannot be realized by natural materials in most situations. Such artificial material is composed of a large amount of periodic metallic units, and its characteristics (e.g., permittivity and permeability) can be easily controlled by changing the geometric parameters of the units [3]. As a result, the study of metamaterials has attracted wide attention in recent years. A great many novel applications have emerged in this domain, including perfect absorption [4, 5], metamaterial sensors [6–9], cloaking [10], Fano effects [11], etc.

The line shape of Fano resonance is quite different from symmetric Lorentzian profile. It is asymmetric and sharp with a relatively high Q-factor. Since Fano theoretically revealed the quantum mechanism of Fano resonance [12], it has become a hot topic. To illustrate the origin of Fano resonance, several theories have been set up, including Fano's quantum mechanical analysis [12], classical oscillator model [13], coupled-mode theory [14], and electromagnetic theory of Fano resonance [15, 16]. According to the electromagnetic theory of Fano

resonance proposed by Gallinet and Martin [16], the distinctive Fano profile is attributed to the coupling between a nonradiative mode and a radiative mode which can also be seen as a continuum.

In terahertz regime, the sharp Fano resonance can be achieved by introducing a weak asymmetry in metamaterials [17–20], which may lead to the appearance of an underlying dark mode [21]. Besides, graphene materials can also be utilized to generate and even modulate the Fano resonance [22, 23]. Compared with a majority of EIT (electromagnetically induced transparency) [24, 25] and PIT (plasmon-induced transparency) [26, 27], Fano line shape is much sharper and narrower. The Q-factor of Fano [17, 28] profile is approximately ten times larger than that of Lorentzian line shape [29–31] in many situations. This property makes Fano resonance a promising choice to realize sensitive detecting [8]. However, the Q-factor of a lot of metamaterials is not high enough [17, 32, 33], which limits their applications in terms of sensing. In order to widely and efficiently apply Fano resonance into sensing, it is a necessary task to greatly improve the Q-factor of a metasurface.

Recently, some metamaterial structures have been designed to realize high-Q Fano resonance. For instance, Ding et al. proposed a bilayer metamaterial which consists of two sets of asymmetric split-rings with different

* Correspondence: wangbenxin@jiangnan.edu.cn
[1]School of Science, Jiangnan University, Wuxi 214122, China
Full list of author information is available at the end of the article

Xie *et al. Nanoscale Research Letters* (2018) 13:294

Page 2 of 7

geometric parameters. It can support three Fano resonances whose Q-factors are respectively 33, 42, and 25 [19]. A symmetric dimer structure composed of identical spit-ring resonators on each layer was also presented to improve its Q-factor [34]. However, these stacked structures are suffering from technical challenges in manufacturing. High-Q resonance with simple structure design still remains to be a hot issue.

In this paper, we demonstrate a coplanar metamaterial structure consisted of four metallic strips. In each unit cell, three parallel strips are arranged perpendicular to the fourth one. This structure can support a high-Q Fano resonance (Q-value is about 58) at 0.81 THz with 25% transmission. This sharp line shape originates from the interaction between bright (radiative) mode and dark (nonradiative) mode. For further discussion, the electromagnetic theory of Fano resonance is employed [15, 16]. The properties of Fano resonance can be changed via controlling of geometric parameters. The sensing performance of the device is discussed. Moreover, by adding more strips into the originally designed structure, multiple Fano resonances can be realized.
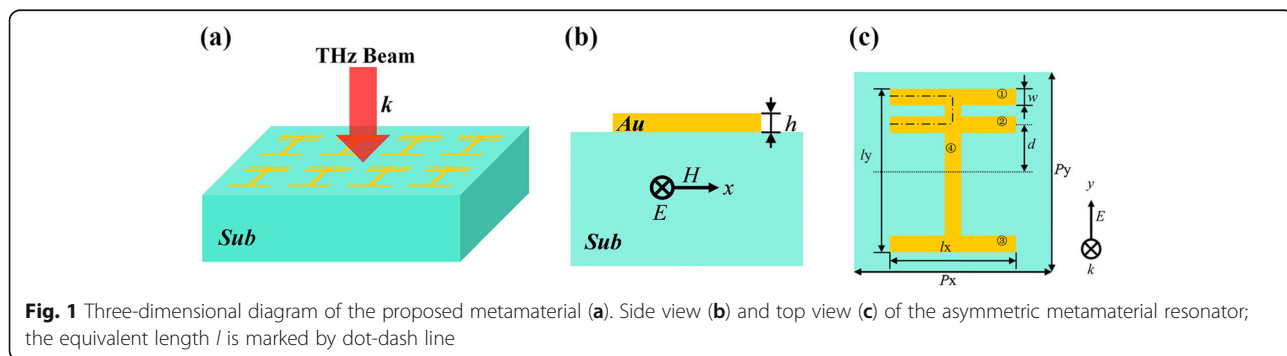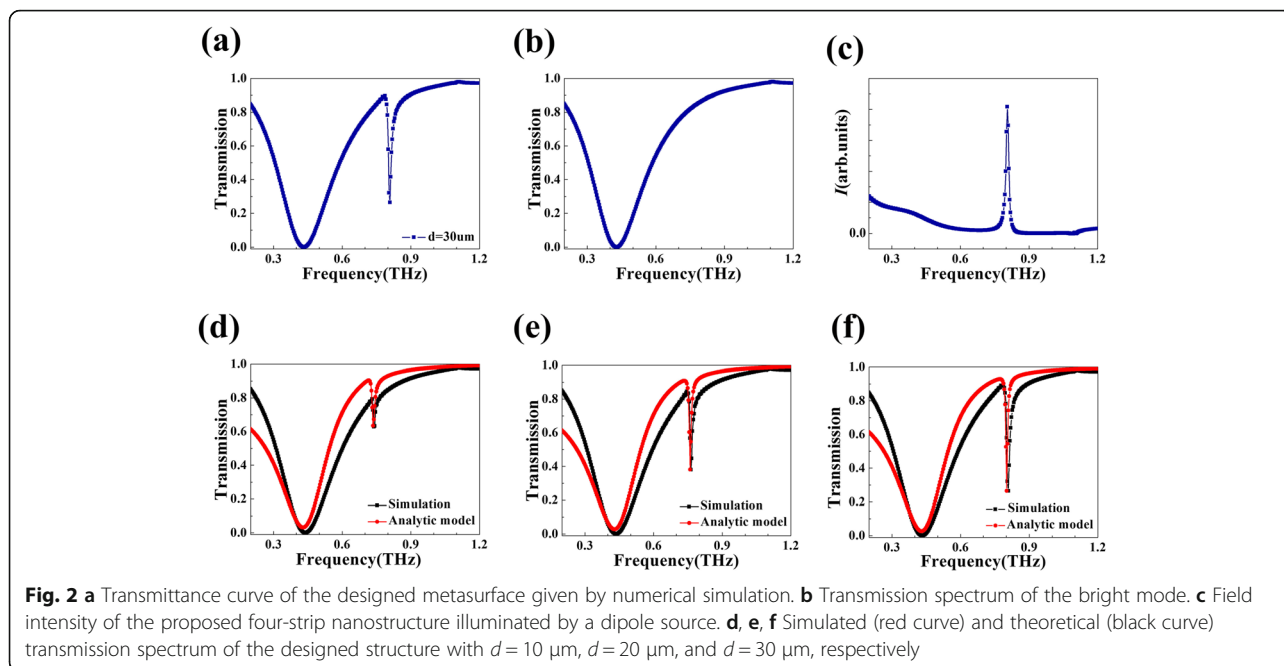
Methods/Experimental

A large amount of researches indicate that breaching the symmetry of a structure may induce an asymmetric Fano line shape [17, 18, 35–37]. Based on this concept, we design this four-strip metamaterial displayed in Fig. 1, where strip 2 is set to realize a symmetry breaking. Figure 1a shows the three-dimensional diagram of the proposed metamaterial. Figure 1b, c respectively shows the side view and top view of the structure unit. The metallic four-strip resonators are placed on the top of an ideal dielectric substrate whose real part of refractive index is 1.5 and imaginary part is 0. In reality, this dielectric material is corresponding to silica. That is to say, the substrate is lossless in terahertz region. We choose Au with conductivity $\sigma = 4.09 \times 10^7$ S/m to form the metallic planar resonator whose thickness is 0.2 μm. The repeat period is $P_x = P_y = 180$ μm. Three parallel strips (1, 2, and 3) have the same size. Their length is $l_x = 120$ μm and width is $w = 20$ μm. Strip 4 is perpendicular to the

other strips (1, 2, and 3). Its length is $l_y = 150$ μm and width is $w = 20$ μm. The distance between the axis of strip 2 and the central point of the structure is $d = 30$ μm. Finite-difference time-domain method is used to simulate this planar metamaterial. In order to save simulation time and computing memory, we choose the mesh sizes of $\Delta x = \Delta y = 1$ μm and $\Delta z = 0.02$ μm. We find the simulation results are quite accurate in this case. Even if smaller mesh sizes are applied, the simulation results are nearly unchanged. The simulating boundary conditions along x-axis and y-axis are set as periodic, and the condition along z-axis is set as perfectly matched layers. Figure 1a shows that the whole structure is illuminated by a beam of normally incident THz wave. As seen in Fig. 1b, c, the electric vector **E** and magnetic vector **H** of the incident THz beam are y-axis polarized and x-axis polarized, respectively.

Results and Discussion

The transmission spectrum of the proposed metasurface is shown in Fig. 2a. There are two transmission dips at the frequencies of 0.430 THz and 0.809 THz with the transmission rates of 0.10% and 26.45%, respectively. In order to make the following explanation more concise, we use R_sR_s and R_d to mark these two resonant modes, R_s for the mode resonant at 0.430 THz and R_d for the resonant mode at a higher frequency. The optical transmission rate of R_s shows a symmetric Lorentz profile with a relatively wide bandwidth of 0.256 THz. By comparison, R_d exhibits an asymmetric Fano line shape which is much sharper with a bandwidth of 0.014 THz. Q-factor is an important criterion to judge the line shape. It can be obtained through dividing the central frequency by bandwidth. In fact, the Q-factor of R_d can reach 58, 30 times more than the Q-value of R_s, which contributes to underlying applications in many fields. The existence of the asymmetric Fano profile roots in the interaction between a dark mode and a bright mode, i.e., the interaction between a nonradiative state and a continuum, generates from a radiative state [16, 38, 39]. In the rest of the paper, detailed mechanism of the Fano line shape will be discussed and theoretical transmission

Fig. 1 Three-dimensional diagram of the proposed metamaterial (**a**). Side view (**b**) and top view (**c**) of the asymmetric metamaterial resonator; the equivalent length *l* is marked by dot-dash line

Xie *et al. Nanoscale Research Letters* (2018) 13:294

Page 3 of 7

Fig. 2 a Transmittance curve of the designed metasurface given by numerical simulation. **b** Transmission spectrum of the bright mode. **c** Field intensity of the proposed four-strip nanostructure illuminated by a dipole source. **d**, **e**, **f** Simulated (red curve) and theoretical (black curve) transmission spectrum of the designed structure with $d = 10$ μm, $d = 20$ μm, and $d = 30$ μm, respectively
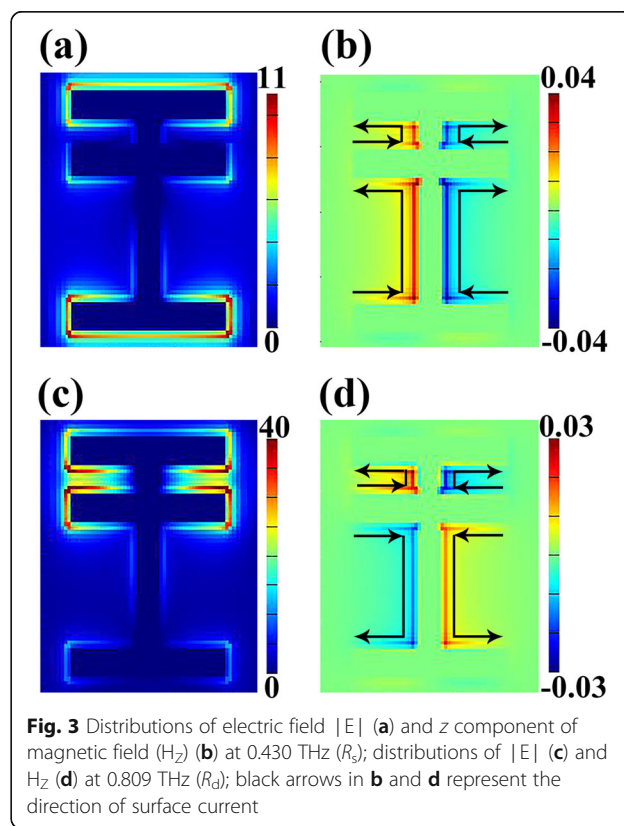
spectra will be analyzed. Although the transmission at 0.809 THz is 26.45% in the proposed metasurface, it can be reduced further. According to [40, 41], the utilization of lossy dielectric materials may reduce transmission. In our simulations, the substrate material we choose is an ideal material with a real refractive index of 1.5 that has no loss in terahertz region. A feasible method to reduce transmission is using a lossy material with a complex refractive index to form the substrate rather than this ideal lossless material.

In order to figure out the origin of the transmittance curve, the distribution of electric field $|\mathbf{E}|$ and the z component of magnetic field (H_Z) at the central frequency of two resonant dips are given in Fig. 3. We can find great differences between the field distributions of R_s and R_d. Figure 3a indicates that the electric field of resonant mode R_s is mainly concentrated on strip 1 and strip 3, especially the ends of these two strips. However, there is very little electric field distribution on other portions of the structure, including strip 2 and strip 4. Such electric field distribution is owing to the electromagnetic field of the normally incident light whose electric vector $\mathbf{E}$ is along y-axis. Therefore, R_s can be regarded as fundamental resonance (i.e., localized electromagnetic EM (electromagnetic) response) [42]. Besides, the distribution of the z component of magnetic field (H_Z) for mode R_s is shown in Fig. 3b from which we can get surface current distribution. It has been demonstrated that analysis of surface current can serve as a vital method to reveal how the coupling of modes generates Fano resonance [28]. As shown in Fig. 3b, surface current flows from the bottom to the upper part of the structure,

contributing to the collection of opposite charges on both sides of strip 1 and strip 3. In contrast, the field distribution at the central frequency of R_d is rather different. Intense electric field is found around strip 1 and strip 2 (Fig. 3c), which is approximately four times larger

Fig. 3 Distributions of electric field $|E|$ (**a**) and z component of magnetic field (H_Z) (**b**) at 0.430 THz (R_s); distributions of $|E|$ (**c**) and H_Z (**d**) at 0.809 THz (R_d); black arrows in **b** and **d** represent the direction of surface current

Xie *et al. Nanoscale Research Letters* (2018) 13:294

Page 4 of 7

than that of the mode R_s. According to the distribution of H_Z field shown in Fig. 3d, it is clear that the surface current flows upwards between strip 1 and strip 2 while the current between strip 2 and strip 3 flows oppositely. At the macro level, such field distribution can be seen as some kind of charge induction between the horizontal strips. From the perspective of mode coupling, this phenomenon is due to the interaction between the bright mode and dark mode.

Aiming to deepen and quantify our explanation, the spectra of bright mode and dark mode are simulated and the electromagnetic theory of Fano resonance [15, 16] is used in the proposed structure. Figure 2b shows the transmission spectrum of a structure whose periodic unit consists of strips 1, 3, and 4. The resonant mode supported by such a structure can be excited directly by plane wave; therefore, it is "bright mode." In contrast, a dark mode cannot be excited by a beam of plane wave; it can be excited through a rapidly varying field, for instance, the near field of a dipole [15, 43]. Figure 2c displays the field intensity of the four-strip metamaterial illuminated by a dipole source [44]. Maxwell's equations form a solid basis of the electromagnetic theory of Fano resonance in nanostructures. According to Maxwell's equations, electric vector *E* obeys the wave equation below:

$$\in^{-1}(\mathbf{r}, \omega) \nabla \times \nabla \times \mathbf{E}(\mathbf{r}, \omega) - \frac{\omega^2}{c^2} \mathbf{E}(\mathbf{r}, \omega) = 0 \tag{1}$$

where ω is the frequency of incident beam and $\in(\mathbf{r}, \omega)$ is the complex dielectric constant of the lossy material. The electric field $\mathbf{E}$ and the permittivity $\in$ are both related to the frequency ω as well as the position vector $\mathbf{r}$. Two orthogonal projection operators P and Q can be used to separate wave function $|E>$ into a bright mode $P|E>$ and a dark mode $Q|E>$, i.e., a radiative mode and a nonradiative mode [15, 38]. Through complicated derivation, the ratio of the total field's strength to the intense of the bright mode can be given as

$$I_a(\omega) = \frac{\left(\frac{\omega^2 - \omega_a^2}{2W_a \omega_a} + q\right)^2 + b}{\left(\frac{\omega^2 - \omega_a^2}{2W_a \omega_a}\right)^2 + 1} \tag{2}$$

where W_a and ω_a are the bandwidth and central frequency of the asymmetric resonance, respectively. The asymmetric parameter q and the modulation damping parameter b are both indispensible to describe $I_a(\omega)$ [15, 16]. The Eq. (2) suggests that $I_a(\omega)$ exhibits an asymmetric profile, which finally results in the asymmetric Fano line shape in the transmittance curve.

The intensity of the bright mode R_s follows a smooth Lorentzian profile. It depends on the frequency ω and obeys the following equation:

$$I_s(\omega) = \frac{a^2}{\left(\frac{\omega^2 - \omega_s^2}{2W_s \omega_s}\right)^2 + 1} \tag{3}$$

of which W_s and ω_s are respectively the bandwidth and central frequency of the spectrum displayed in Fig. 2b, and a is the maximum value of the resonance's amplitude. The total strength $I(\omega)$ of the resonance can be calculated by the product of I_a and I_s, from which we can finally get the transmittance $T(\omega)$.
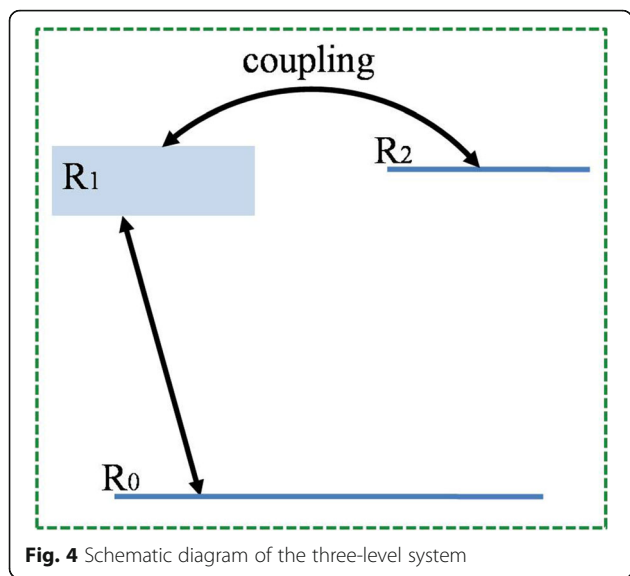
$$I(\omega) = I_a(\omega) \times I_s(\omega) \tag{4}$$

$$T(\omega) = 1 - I(\omega) \tag{5}$$

In order to meet the requirement of energy conservation, a should not be greater than 1. W_a and ω_a can be calculated from the central frequency and bandwidth [15, 16]. The asymmetric parameter q as well as the modulation damping parameter b can be obtained through the method given by [16]. In this way, we can get the theoretical transmission spectrum of this asymmetric structure. In Fig. 2f, the black curve represents the transmission spectrum given by FDTD method and the red curve gives the results of our calculation based on electromagnetic theory of Fano resonance. The consistent trend of black and red curve indicates that it is reasonable to attribute the resonator's transmission characteristics to the coupling of the bright mode and dark mode. This conclusion also coincides with the distribution of field in Fig. 3.

The geometric parameter d describes the distance between the axis of strip 2 and the central point of the whole structure (Fig. 1c). It can greatly affect the central frequency of transmission dips as well as their transmission coefficients. Corresponding transmission spectra with different d are shown in Fig. 2d, e. The black curve and red curve represent the transmission spectrum based on simulation and theoretical calculation, respectively. With d changing from 10 to 30 μm, it is clear that a sharp Fano dip deepens, resulting from the increasing coupling strength between the bright mode and dark mode. Furthermore, the central frequency of the mode R_d exists a distinct blue shift when strip 2 is placed closer to strip 1. Based on LC circuit model, the resonance frequency of R_d is given by [45].

$$\omega_d = \frac{1}{2\pi\sqrt{LC/2}} \propto \frac{1}{l} \tag{6}$$

where l is the equivalent length of the corresponding resonator. Equation (6) indicates that the central frequency ω_d is in inverse proportion to l. In our structure, equivalent length l is indicated by the length of dot-dash line in Fig. 1c. This is because the field distributions of R_d are mainly restricted to the strip 1 and 2. The length
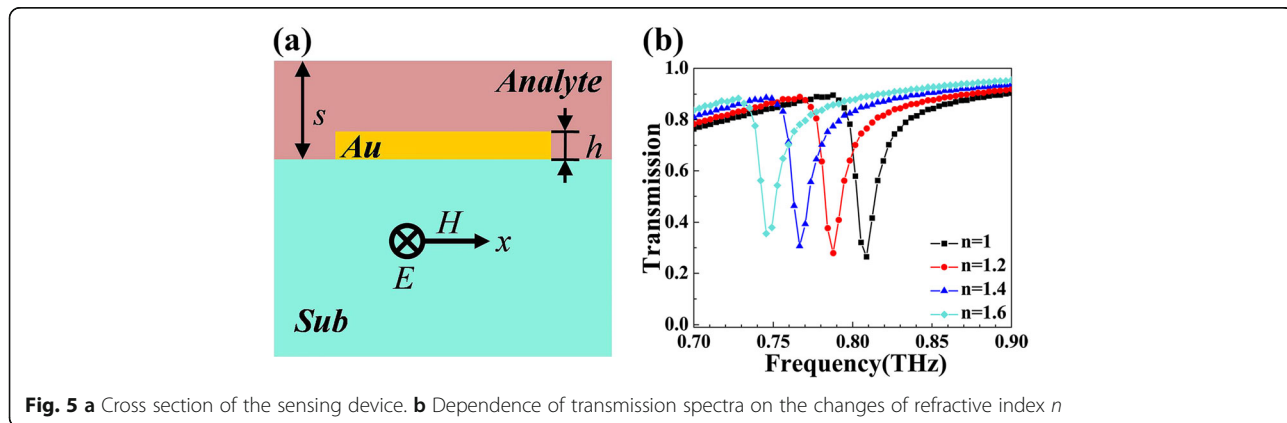
Xie *et al. Nanoscale Research Letters* (2018) 13:294

Page 5 of 7

Fig. 4 Schematic diagram of the three-level system

of strip 1 (and 2) and the distance between the two strips together decide l. When d increases, the distance between the two strips declines. Hence, as shown in Fig. 1c, the equivalent length decreases when d changes from 10 to 30 μm. This leads to the increase of R_d's resonant frequency.
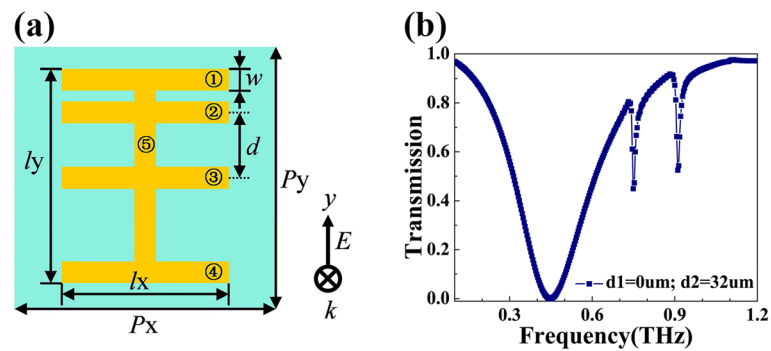
According to the theory of Fano resonance suggested by Fano in 1961 [12], the process of autoionization is studied and the asymmetric line shape of the resonance is attributed to the interference between a continuum and a discrete state. This is also the origin of those asymmetric characteristics of the metamaterial resonator presented in this paper. As shown in Fig. 4, a three-level system can be utilized to clarify the transition mechanism of the structure. R_0 serves as the ground state of the whole system. Bright mode R_1 is a radiative mode that can be directly excited by the normally incident beam. In this system, the nonradiative state R_2 can be regarded as a "dark mode" [21] as discussed before. R_2 can be

excited through the symmetry breaking. Introducing an asymmetry offers a channel to allow the bright mode to couple with the dark mode, and therefore, leads to the Fano resonance [46].

The strong interaction between incident electromagnetic wave and the analyte layer makes high-Q Fano resonance, a promising method to realize ultra-sensitive detecting of refractive index n [8]. The device proposed in Fig. 5a can function as an effective sensor to detect the refractive index n of the analyte layer on the top whose thickness is 4 μm. The central frequency of the Fano dip will change with the change of n. Therefore, we can get the refractive index by analyzing the resonant frequency of R_d. Figure 5b shows the shift of Fano dip's resonant frequency in the device. A distinct red shift appears when n is increased from 1 to 1.6. The sensing sensitivity S is equal to $\frac{\Delta f}{\Delta n}$. Here, S of the sensor is calculated to be 0.105 THz/RIU (refractive index unit). It is well known that FOM (Figure of merit) is a vital criterion for the performance of a sensor [47]. It can be calculated by FOM = $\frac{S}{\text{linewidth}}$. In this presented structure, the FOM value can reach 7.501, which is on an ideal level [47, 48]. The sensing capability is also usually discussed by FOM* = $\frac{S^*}{I}$ and S* = $\frac{\Delta I}{\Delta n}$, which is related to the detected intensity. The calculation result of S* in this structure is 2.6/RIU. And the FOM* in our structure is calculated to be 10. We also did some work to figure out the variation of the response with the thickness of the analyte layer. Please refer to the Additional file 1.

Multiple Fano resonances could have applications in many situations. However, most of the plasmonic Fano metamaterials are designed to support single Fano resonance [11, 17]. Therefore, it is not easy for them to realize multiple Fano resonances through the adjustment of structure. In this paper, we realize multiple Fano resonances by adding more horizontal strips into the original design of the metamaterial. We present a five-strip structure as a representative example. The schematic

Fig. 5 a Cross section of the sensing device. **b** Dependence of transmission spectra on the changes of refractive index n

Xie *et al. Nanoscale Research Letters* (2018) 13:294

Page 6 of 7

Fig. 6 a Top view of the proposed five-strip structure. **b** Simulated transmittance curve of the five-strip resonator

diagram of the five-strip resonator is shown in Fig. 6a. Strips 1, 2, 3, and 4 are in the same size and parallel to each other. Their length is $l_x = 120$ μm and width is $w = 20$ μm. Strip 3 is located in the middle, and the distance d between the axes of strip 2 and strip 3 is 32 μm. Strip 5 is perpendicular to the other four strips. Its length is $l_y = 150$ μm and width is $w = 20$ μm. The boundary conditions and mesh size are kept the same as the simulation of four-strip resonator. The simulation result is shown in Fig. 6b, in which we can clearly find two sharp Fano dips at 0.75 THz and 0.91 THz. The Q values of these two dips are respectively 61 and 65. More Fano dips should be generated if more horizontal strips are added into the structure.

Conclusion

In conclusion, we design a four-strip planar resonator which can support sharp Fano resonance with a high Q-value. The bandwidth of the Fano dip is 0.014 THz and its Q-factor is 58. The interaction between bright mode and dark mode results in the appearance of the asymmetric Fano profile. The theoretical transmission spectrum is calculated in this paper. Furthermore, multiple high-Q Fano resonances can be realized by adding more horizontal strips to the structure. This structure can be applied in sensing and other fields.

Additional File

Additional file 1: The variation of the response with the thickness of the analyte layer. (DOCX 297 kb)

Abbreviations

EIT: Electromagnetically induced transparency; EM: Electromagnetic; FOM: Figure of merit; PIT: Plasmon-induced transparency; Q: Quality factor; RIU: Refractive index unit

Availability of Data and Materials

All data are fully available without restriction.

Authors' Contributions

BXW conceived the research and supervised the whole work. QX and GXD conducted the simulations and analyses and wrote the manuscript. WQH assisted in processing the data and figures. All authors read and approved the final manuscript.

Competing Interests

The authors declare that they have no competing interests.

Publisher's Note

Springer Nature remains neutral with regard to jurisdictional claims in published maps and institutional affiliations.

Author details

[1]School of Science, Jiangnan University, Wuxi 214122, China. [2]School of Physics and Electronics, Hunan University, Changsha 410082, China.

References

1. Smith DR, Padilla WJ, Vier DC, Nemat-Nasser SC, Schultz S (2000) Composite medium with simultaneously negative permeability and permittivity. Phys Rev Lett 84:4184
2. Choi M, Lee SH, Kim Y, Kang SB, Shin J, Kwak MH, Kang KY, Lee YH, Park N, Min B (2011) A terahertz metamaterial with unnaturally high refractive index. Nature 470:369–373
3. Pendry JB, Martín-Moreno L, Garcia-Vidal FJ (2004) Mimicking surface plasmons with structured surfaces. Science 305:847–848
4. Landy NI, Sajuyigbe S, Mock JJ, Smith DR, Padilla WJ (2008) Perfect metamaterial absorber. Phys Rev Lett 100:207402
5. Liu N, Mesch M, Weiss T, Hentschel M, Giessen H (2010) Infrared perfect absorber and its application as plasmonic sensor. Nano Lett 10:2342–2348
6. Singh R, Cao W, Al-Naib I, Cong L, Withayachumnankul W, Zhang WL (2014) Ultrasensitive terahertz sensing with high-Q Fano resonances in metasurfaces. Appl Phys Lett 105:171101
7. Xu WD, Xie LJ, Ying YB (2017) Mechanisms and applications of terahertz metamaterial sensing: a review. Nanoscale 9:13864–13878
8. Jaksic Z, Vukovic S, Matovic J, Tanaskovic D (2010) Negative refractive index metasurfaces for enhanced biosensing. Materials. 4:1–36
9. Yu P, Wu J, Ashalley E, Govorov AO, Wang ZM (2016) Dual-band absorber for multispectral plasmon-enhanced infrared photodetection. J Phys D Appl Phys 49:365101
10. Schurig D, Mock JJ, Justice BJ, Cummer SA, Pendry JB, Starr AF, Smith DR (2006) Metamaterial electromagnetic cloak at microwave frequencies. Science 314:977–980
11. Al-Naib I (2018) Thin-film sensing via Fano resonance excitation in symmetric terahertz metamaterials. J Infrared Millim Terahertz Waves 39:1–5

Xie *et al. Nanoscale Research Letters* (2018) 13:294

Page 7 of 7

12. Fano U (1961) Effects of configuration interaction on intensities and phase shifts. Phys Rev Lett 124:1866
13. Joe YS, Satanin AM, Kim CS (2006) Classical analogy of Fano resonances. Phys Scr 74:259
14. Ruan Z, Fan S (2010) Temporal coupled-mode theory for Fano resonance in light scattering by a single obstacle. J Phys Chem C 114:7324–7329
15. Gallinet B, Martin OJF (2011) Ab initio theory of Fano resonances in plasmonic nanostructures and metamaterials. Phys Rev B 83:235827
16. Gallinet B, Martin OJF (2011) Influence of electromagnetic interactions on the line shape of plasmonic Fano resonances. ACS Nano 5:8999–9008
17. Singh R, Al-Naib I, Koch M, Zhang WL (2011) Sharp Fano resonances in THz metamaterials. Opt Express 19:6312–6319
18. Cao W, Singh R, Ai-Naib I, He M, Taylor AJ, Zhang WL (2012) Low-loss ultra-high-Q dark mode plasmonic Fano metamaterials. Opt Lett 37:3366–3368
19. Ding CF, W L, Xu DG, Yao JQ, Sun XH (2016) Triple-band high Q factor Fano resonances in bilayer THz metamaterials. Opt Commun 370:116–121
20. Xiao X, Wu JB, Miyamaru F, Zhang MY, Li SB, Takeda MW, Wen WJ, Sheng P (2011) Fano effect of metamaterial resonance in terahertz extraordinary transmission. Appl Phys Lett 98:011911
21. Fedotov VA, Rose M, Prosvirnin SL, Papasimakis N, Zheludev NI (2007) Sharp dark-mode resonances in planar metamaterials with broken structural symmetry. Phys Rev Lett 99:12243–12254
22. He XY, Lin FT, Liu F, Shi WZ (2016) Terahertz tunable graphene Fano resonance. Nanotechnology 27:485202
23. Xiao SY, Wang T, Jiang XY, Yan XC, Cheng L, Wang BY, Xu C (2017) Strong interaction between graphene layer and Fano resonance in terahertz metamaterials. J Phys D 50:195101
24. Lu XQ, Shi JH, Liu R, Guan CY (2012) Highly-dispersive electromagnetic induced transparency in planar symmetric metamaterials. Opt Express 20: 17581–17590
25. Liao Z, Liu S, Ma HF, Li C, Jin BB, Cui TJ (2016) Electromagnetically induced transparency metamaterial based on spoof localized surface plasmons at terahertz frequencies. Sci Rep 6:27596
26. Xu Q, Su XQ, Ouyang CM, Xu NN, Cao W, Zhang YP, Li Q, Hu C, Gu JQ, Tian Z, Azad AK, Han JG, Zhang WL (2016) Frequency-agile electromagnetically induced transparency analogue in terahertz metamaterials. Opt Lett 41:4562–4565
27. Zhang XQ, Li Q, Cao W, Gu JQ, Singh R, Tian Z, Han JG, Zhang WL (2013) Polarization-independent plasmon-induced transparency in a fourfold symmetric terahertz metamaterial. IEEE J Sel Top Quantum Electron 19: 8400707
28. Chen Y, Chu JR, Xu XF (2016) Plasmonic multibowtie aperture antenna with Fano resonance for nanoscale spectral sorting. ACS Photonics 3:1689–1697
29. Chowdhury DR, Singh R, Reiten M, Chen HT, Taylor AJ, O'Hara JF, Azad AK (2011) A broadband planar terahertz metamaterial with nested structure. Opt Express 19:15817–15823
30. Dong GX, Xie Q, Zhang Q, Wang BX, Huang WQ (2018) Plasmon-induced transparency based on triple arc-rings. Materials 11:964
31. Park SJ, Yoon SAN, Ahn YH (2016) Dielectric constant measurements of thin films and liquids using terahertz metamaterials. RSC Adv 6:73
32. Singh R, Al-Naib I, Cao W, Rockstuhl C, Koch M, Zhang WL (2013) The Fano resonance in symmetry broken terahertz metamaterials. IEEE Trans Terahertz Sci Technol 3:820–826
33. Li Q, Cong LQ, Singh R, Xu NN, Cao W, Zhang XQ, Tian Z, Du LL, Han JG, Zhang WL (2016) The monolayer graphene sensing enabled by the strong Fano resonant metasurface. Nanoscale 8:17278–17284
34. Du LH, Li J, Liu Q, Zhao JH, Zhu LG (2017) High-Q Fano-like resonance based on asymmetric dimer structure and its terahertz sensing application. Opt Mater Express 7:1335–1342
35. Cong LQ, Manjappa M, Xu NN, Al-Naib I, Zhang WL, Singh R (2015) Fano resonances in terahertz metasurfaces: a figure of merit optimization. Adv Opt Mater 3:1537–1543
36. Nguyen TK, Le TD, Dang PT, Le KQ (2017) Asymmetrically engineered metallic nanodisk clusters for plasmonic Fano resonance generation. J Opt Soc Am B 34:668–672
37. Li XF, Bian XY, Milne WI, Chu DP (2016) Fano resonance engineering in mirror-symmetry-broken THz metamaterials. Appl Phys B 122:95
38. Feshbach H (1958) A unified theory of nuclear reactions. Ann Phys 5:357–390
39. Zhang W, Govorov AO, Bryant GW (2006) Semiconductor-metal nanoparticle molecules: hybrid excitons and the nonlinear Fano effect. Phys Rev Lett 97:146804
40. Yu P, Besteiro LV, Wu J, Huang YJ, Wang YQ, Govorov AO, Wang ZM (2018) Opt Express 26:20471–20480
41. Xie Q, Dong GX, Wang BX, Huang WQ (2018) Design of quad-band terahertz metamaterial absorber using a perforated rectangular resonator for sensing applications. Nanoscale Res Lett 13:137
42. Wang BX, Xie Q, Dong GX, Zhu HX (2017) Broadband terahertz metamaterial absorber based on coplanar multi-strip resonators. J Mater Sci 28:17215–17220
43. Zhang WL, Gallinet B, Martiin OJF (2010) Symmetry and selection rules for localized surface plasmon resonances in nanostructures. Phys Rev B 81:233407
44. Martin OJF, Girard C (1999) Generalized field propagator for arbitrary finite-size photonic band gap structures. Phys Rev Lett 82:315–318
45. Wang BX, Wang LL, Wang GZ, Huang WQ, Li XF, Zhai X (2013) A simple design of ultra-broadband and polarization insensitive terahertz metamaterial absorber. Appl Phys A 115:1187–1192
46. Han S, Singh R, Cong LQ, Yang HL (2014) Engineering the Fano resonance and electromagnetically induced transparency in near-field coupled bright and dark metamaterial. J Phys D 48:035104
47. Zhang YP, Li TT, Zeng BB, Zhang HY, Lv HH, Huang XY, Zhang WL, Azad AK (2015) A graphene based tunable terahertz sensor with double Fano resonances. Nanoscale 7:12682–12688
48. Ye J, Dorpe PV (2011) Improvement of figure of merit for gold nanobar array plasmonic sensors. Plasmonics 6:665–671